Dose dependence of Cu precipitate formation in Fe-Cu model alloys irradiated with fission neutrons

AUTHOR(S):

Xu, Q; Yoshiie, T; Sato, K

CITATION:

Xu, Q ...[et al]. Dose dependence of Cu precipitate formation in Fe-Cu model alloys irradiated with fission neutrons. PHYSICAL REVIEW B 2006, 73(13): 134115.

ISSUE DATE:

2006-04

URL:

http://hdl.handle.net/2433/39881

PHYSICAL REVIEW B **73**, 134115 (2006)

Dose dependence of Cu precipitate formation in Fe-Cu model alloys irradiated with fission neutrons

Q. Xu, T. Yoshiie, and K. Sato
Research Reactor Institute, Kyoto University, Osaka 590-0494, Japan
(Received 12 November 2004; revised manuscript received 27 December 2005; published 26 April 2006)

The formation of Cu precipitates was investigated in two Fe-Cu binary model alloys irradiated at 573 K with fission neutrons at doses from 4×10^{-4} to 6×10^{-3} displacement per atom (dpa). Experimental positron annihilation results indicated that Cu precipitates were formed even after irradiation to 4×10^{-4} dpa. Microvoids formed and grew at the Cu precipitates upon irradiation from 4×10^{-4} to 3×10^{-3} dpa. These microvoids shrank and a prominent aggregation of Cu atoms occurred upon irradiation from 3×10^{-3} to 6×10^{-3} dpa. The formation processes of Cu precipitates and microvoids were simulated on the basis of a rate theory. The results indicate that Cu precipitates are formed first, follow by the generation of microvoids at the Cu precipitates as Cu cluster-vacancies complexes, which agree qualitatively with the experimental results.

DOI: 10.1103/PhysRevB.73.134115 PACS number(s): 61.82.Bg, 78.70.Bj, 81.30.Mh

I. INTRODUCTION

Cu atoms are almost insoluble in α-Fe. Cu precipitates form in Fe-Cu alloys not only during thermal aging at high temperatures, but also upon irradiation with high-energy particles.[1,2] The formation of Cu-rich precipitates during neutron irradiation is considered a key factor influencing the radiation-induced embrittlement observed in old commercial reactor pressure vessel (RPV) steels, and this phenomenon has been extensively investigated.[1–4] Cu precipitates obstruct the dislocation motion during deformation, increasing hardness and decreasing ductility, and thus induce embrittlement. Therefore, both the concentration and the size of Cu precipitates are important factors for the embrittlement of RPV steels. It has been found that in thermally aged and neutron irradiated model Fe-Cu alloys, the evolution of precipitates is an Ostwald ripening process.[1] An important feature of this process is that with increasing size, Cu precipitates change from a body- (bcc) to a face-centered-cubic (fcc) structure following the phase transformations bcc $\rightarrow$ 9R $\rightarrow$ 3R $\rightarrow$ fcc.[2,5] Nagai *et al.*[6] recently reported that Cu atoms aggregate on microvoid surfaces during annealing. It is well known that the Cu atoms aggregate by a vacancy mechanism.[7] However, the relationship between the formation of microvoids and Cu precipitates under irradiation remains unclear. The main purpose of the present study was to investigate the mechanism of nucleation and growth of Cu precipitates under irradiation. Special attention was paid to the effect of microvoid formation on the growth of Cu precipitates in the initial stage of irradiation.

Generally, transmission electron microscopy has been used to investigate the formation of copper precipitates.[2] However, direct observation of small Cu precipitates in Fe-Cu alloys is difficult due to the high magnetism. Atom probe field ion microscopy offers an alternative method,[8,9] but only small areas can be observed by this technique.

Positron annihilation spectroscopy is a powerful tool for detecting vacancy-type defects in condensed matter.[10] Doppler broadening of positron annihilation radiation is a nondestructive technique for testing defect clusters. In the dominant decay mode of a thermal positron and electron, two gamma rays are emitted. In the laboratory frame, the energy of two photons emitted by the annihilation of a positron and electron is different. The difference in photon energy is proportional to the longitudinal component of the electron-positron momentum in the direction of gamma emission. From a measurement of photon energies, information about the momentum distribution of core electrons can be obtained. Therefore, Doppler-broadening measurements can provide useful information about the distribution of elements around the annihilation site. Recently, Doppler-broadening measurements were improved by a two-Ge-detector coincidence system, which makes the background of high momentum contributions decrease by about two or three orders of magnitude compared with traditional measurements using a single Ge detector.[11]

In the present study, the positron lifetime and coincidence Doppler broadening (CDB) methods were used to measure the defects in neutron irradiated Fe-Cu alloys.

II. EXPERIMENTAL PROCEDURE

Two Fe-Cu alloys, namely Fe-0.3Cu and Fe-0.6Cu, were tested in this study, where the composition of Cu is in weight percent. The model alloys were prepared from pure Fe (99.99%) and copper (99.9%) using a high-frequency induction furnace in a vacuum. After melting, solution treatment was carried out at 1423 K for 24 h, followed by quenching in water. All specimens were rolled to a thickness of 0.2 mm, punched into 5 mm disks, annealed at 1223 K for 0.5 h in a vacuum, and quenched in water. The neutron irradiations were carried out at the Kyoto University Reactor (Ref. 12) at a constant temperature of 573 K from 10 to 136 h with a neutron flux of 5.5×10^{16} n/m^{2}s ($E>1$ MeV). The total irradiation doses ranged from 2×10^{21} to 2.7×10^{22} n/m^2, which corresponds to 4×10^{-4} to 6×10^{-3} displacement per atom (dpa) if the threshold energy of Fe is assumed to be 24 eV. To compare the formation of microvoids in Fe-Cu alloys and pure Fe, well-annealed Fe was irradiated at the Japan Material

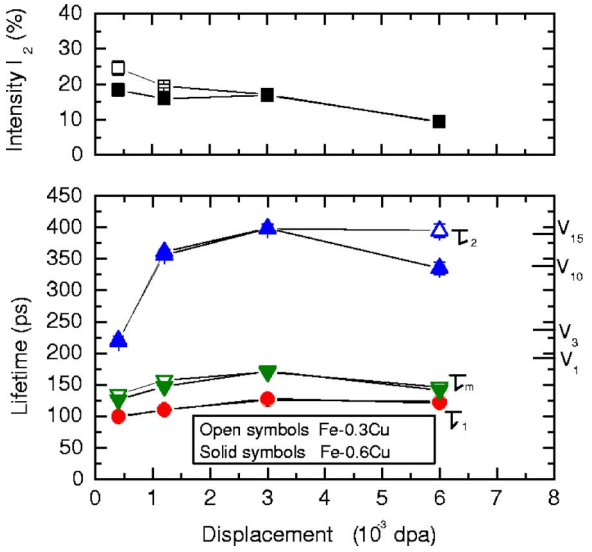

FIG. 1. (Color online) Positron lifetimes and intensities of long lifetime in irradiated Fe-0.3Cu and Fe-0.6Cu.

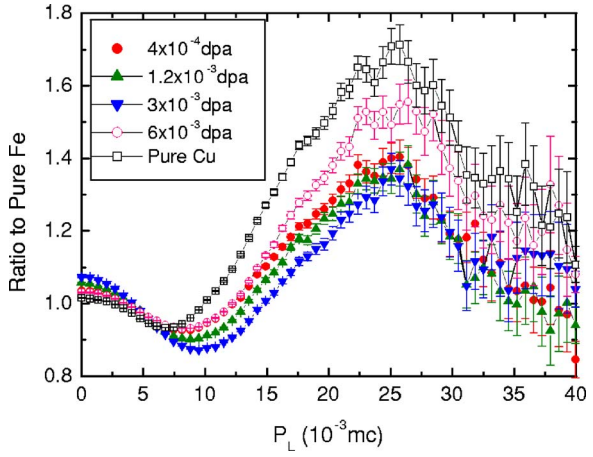

FIG. 2. (Color online) Typical CDB ratio curves of irradiated Fe-0.6Cu and pure Cu to unirradiated pure Fe.

Testing Reactor (JMTR), where the irradiation temperature was 563 K, and the doses were 3.9×10^{22} n/m^2, 1.8×10^{23} n/m^2, 3×10^{23} n/m^2, and 8.2×10^{23} n/m^2, corresponding to 9.6×10^{-3} dpa, 4.4×10^{-2} dpa, 7.4×10^{-2} dpa, and 0.2 dpa, respectively. Positron lifetime and CDB were measured at room temperature before and after irradiation. The positron lifetime spectrometer had a time resolution of 190 ps (full width at half maximum) and each spectrum was accumulated to a total of 1×10^6 counts. To discriminate between bulk and defect components, after subtracting the source and background components, a lifetime spectrum $L(t)$ was decomposed into two components using the programs RESOLUTION and POSITRONFIT[13]:

$$L(t) = (I_1/\tau_1)\exp(-t/\tau_1) + (I_2/\tau_2)\exp(-t/\tau_2), \qquad (1)$$

where τ_i are the lifetimes and I_i are the intensities. The long lifetime τ_2 comes from vacancies and vacancy clusters, and the short lifetime τ_1 results from positron lifetime of free electrons and other defects, such as dislocations.

The average positron lifetime τ_m is defined as:

$$\tau_m = I_1\tau_1 + I_2\tau_2. \qquad (2)$$

Doppler-broadening spectra were accumulated to a total of 2×10^7 counts. The energy resolution was 1.4 keV at 511 keV.

III. RESULTS

A. Lifetime measurements

Figure 1 shows the lifetimes and intensities of irradiated Fe-0.3Cu and Fe-0.6Cu. The calculated positron lifetimes of V_1 (single vacancy), V_3 (trivacancies), V_{10} (ten vacancies), and V_{15} (fifteen vacancies) in pure Fe by Puska *et al.*[14] using the superposition method are also shown in the figure. After irradiation to 4×10^{-4} dpa, the long lifetime τ_2 was 220.5 ps with an intensity of 24.6% and 218.8 ps with an intensity of 18.4% in Fe-0.3Cu and Fe-0.6Cu, respectively, which corresponds to a V_3. The long lifetime τ_2 increased to 399 ps, which meant that the microvoids grew in both alloys during irradiation from 4×10^{-4} to 3×10^{-3} dpa. The lifetime of 399 ps corresponds to the microvoid V_{15}. When the irradiation dose increased from 3×10^{-3} to 6×10^{-3} dpa, the long lifetime τ_2 (394.9 ps) changed little in Fe-0.3Cu, whereas it decreased to 335.5 ps in Fe-0.6Cu. The intensity I_2 of microvoids decreased slightly during irradiation.

The results also show that the lifetimes at any given irradiation dose were almost the same in the two alloys except at 6×10^{-3} dpa, which will be discussed later. This means that the mechanism of formation of microvoids is largely the same in the two alloys at the present irradiation doses. Nagai *et al.*[6] reported different lifetime results for nominally the same Fe-0.3Cu alloy irradiated at the Irradiation Facility of Hydraulic Rabbit II of the JMTR, where the long lifetime τ_2 was 300 ps with an intensity of 30%, and the short lifetime τ_1 was 160 ps. The fast neutron fluence (8.3×10^{22} n/m^2) was higher than that in the present study (2.7×10^{22} n/m^2), and the neutron flux of the JMTR was about three times higher than that in the present study. In addition, the key difference was the temperature control during irradiation. In the present study, the specimen temperature was controlled accurately with an electric heater and helium pressure. The variation of irradiation temperature was the most important factor affecting the formation of vacancy clusters.[15,16]

B. CDB measurement

Figure 2 shows typical ratio curves of irradiated Fe-0.6Cu to unirradiated pure Fe. In order to identify Cu precipitates, the ratio curve of pure Cu to pure Fe is also shown in the figure. After irradiation, ratio curves were higher than 1 in the low momentum region because more positrons were annihilated by valence electrons at vacancies in the irradiated samples. In addition, the ratio curve of pure Cu shows a peak at about 25×10^{-3} m_0c, where m_0 is the electron rest mass, and c is the velocity of light. There were peaks at the same position in the case of irradiated Fe-0.6Cu alloys, and these

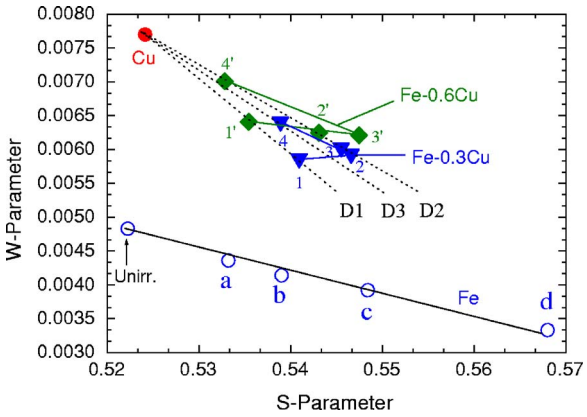

FIG. 3. (Color online) Irradiation dose dependence of the S-W plot. The points (1,1′), (2,2′), (3,3′), and (4,4′) correspond to an irradiation dose of 4×10^{-4}, 1.2×10^{-3}, 3×10^{-3}, and 6×10^{-3} dpa in Fe-0.3Cu and Fe-0.6Cu, respectively. The irradiation doses were higher in Fe than those in the Fe-Cu alloys. (a)–(d) represent an irradiation dose of 9.6×10^{-3}, 4.4×10^{-2}, 7.4×10^{-2}, and 0.2 dpa in JMTR at 563 K. "Unirr." represents unirradiated Fe.

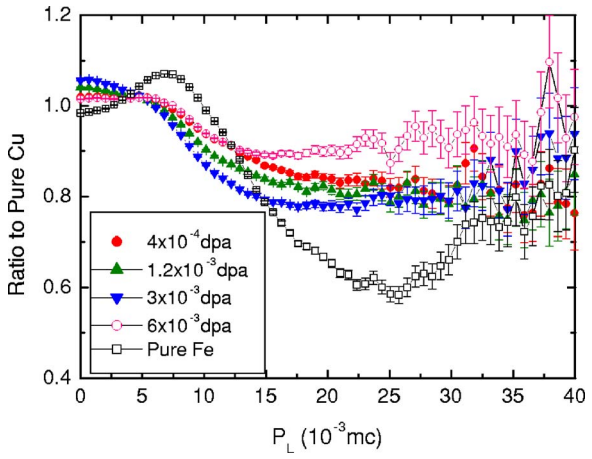

FIG. 4. (Color online) Typical CDB ratio curves of irradiated Fe-0.6Cu and pure Fe to unirradiated pure Cu.

came from Cu precipitates.[17] In the present study, we introduced two parameters, namely S and W, defined as the ratio of the low-momentum ($|P_L|<4\times10^{-3}\ m_0c$) and high-momentum ($20\times10^{-3}\ m_0c<|P_L|<30\times10^{-3}\ m_0c$) regions in the Doppler-broadening spectrum to the total region, respectively. S represents the smaller Doppler shift resulting from the annihilation of valence electrons. In the same materials, the increase in S compared with a well-annealed sample comes from the annihilation at vacancy-type defects. W comes from the annihilation at core electrons, which is used to estimate the number of Cu atoms around positrons when they are annihilated. The correlation between Cu precipitation and microvoid formation is shown in Fig. 3, where our data for unirradiated pure Cu and Fe and those for irradiated Fe are shown. The data for irradiated Fe were obtained by the irradiation at the JMTR at 563 K. The irradiation doses in Fe were higher than those used in the case of the Fe-Cu alloys, since no microvoids were formed and no changes occurred in S and W in Fe in the latter case. Even after irradiation to 4×10^{-4} dpa, Cu precipitates formed in both alloys since W was larger than that of unirradiated Fe. Microvoids also formed in both alloys as revealed by the lifetime and CDB results. In the Fe-0.3Cu alloy, with increasing irradiation dose, first both S and W increased, although the increase of W was not prominent from 4×10^{-4} to 1.2×10^{-3} dpa, and then W continued to increase but S decreased. Compared with the lifetime results described above, the increase in S corresponded to the growth of microvoids, while the subsequent decrease in S corresponded to a decrease in the microvoid concentration. The variation of S with irradiation dose was the same in Fe-0.6Cu as in Fe-0.3Cu, i.e., S increased with an increasing irradiation dose from 4×10^{-4} to 3×10^{-3} dpa. According to the lifetime results, the increase of S corresponded to the growth of microvoids, whereas the variation of W with irradiation dose was somewhat different from that in Fe-0.3Cu; namely, W decreased slightly with increasing irradiation dose from 4×10^{-4} to 3×10^{-3} dpa. With the increasing growth of microvoids, the fraction of positron annihilation in valence electrons at microvoids increased. However, the fraction of positron annihilation in core electrons of Cu decreased because the affinity for vacancies was high. Thus, aggregation of Cu did not increase W. As in the case of Fe-0.3Cu, S decreased and W increased when the irradiation dose exceeded 6×10^{-3} dpa. According to the lifetime results, the decrease in S was caused by a decrease in size and concentration of microvoids. The increase in W was indicative of increased Cu aggregation.

In Fig. 3, the (S, W) points (1,1′), (2,2′), and (4,4′) were aligned on the same line segment formed by D1, D2, and D3, which went through the (S_{Cu},W_{Cu}) point corresponding to the annihilation in pure Cu. This indicated that a fraction of the positrons was annihilated at Cu precipitates and another fraction at the microvoids. The points 1′, 2′, and 3′, were closer to the (S_{Cu},W_{Cu}) point, indicating that the fraction of annihilation at the Cu precipitates is higher in the Cu-rich alloy. The slope of D2 was higher than that of D1, indicating that the free volume of the microvoids detected at the irradiation dose of 1.2×10^{-3} dpa was larger than that of 4×10^{-4} dpa as shown in the lifetime results of Fig. 1. The slope increased with the increase in free volume of the microvoids and decreased with the decrease in free volume. The point (S_{Cu},W_{Cu}), (3,3′), was not on the same straight line. This contradiction will be explained in the discussion section.

The clustering process of Cu and vacancies was different before and after irradiation [1.2×10^{-3} dpa (Fe-0.3Cu) and 3×10^{-3} dpa (Fe-0.6Cu)]. In order to investigate the relationship between the microvoids and Cu precipitates, CDB results of Fe-Cu alloys were compared with that of pure Cu. Figure 4 shows typical ratio curves of pure Fe and irradiated Fe-0.6Cu to unirradiated pure Cu. The ratio curve of pure Fe shows a big valley, and a peak at about $25\times10^{-3}\ m_0c$. In irradiated Fe-0.6Cu, however, the ratio curves were almost flat in the high-momentum ($>15\times10^{-3}\ m_0c$) region. This indicated that the positrons did not annihilate with core electrons in Fe in irradiated Fe-Cu alloys. As the affinity of positrons is higher for microvoids than for Cu precipitates, the positrons trapped at microvoids were annihilated with core electrons in Cu.

C. Rate theory analysis

In order to investigate the Cu precipitation mechanism in detail, computer simulations were performed using a simple model based on the rate theory. Following Odette's model,[7] it is assumed that the diffusion of Cu atoms occurs by a vacancy mechanism and that the Cu clusters are homogeneously nucleated. In addition, interstitial and vacancy defect clusters are assumed to form by the migration of single interstitials and vacancies. Cu clusters, where two Cu atoms are assumed to be the nucleus of a cluster, are sinks for vacancies, but not for interstitials. The variation of the concentration of interstitials C_I is expressed by the following equation:

$$dC_I/dt = P - Z_{IV}C_IC_V(M_I + M_V) - 2Z_{II}M_IC_I^2 - Z_{LI}M_IC_I(C_LC_{LI})^{1/2} - Z_{\mathrm{Void}I}M_IC_I(C_{\mathrm{Void}}C_{\mathrm{VoidV}})^{1/3} - Z_{I\mathrm{Cu}}M_IC_I(C_{\mathrm{CuV}} + C_{C\mathrm{CuV}}) - Z_{SI}M_IC_IC_S, \quad (3)$$

where P is the production rate of Frenkel pairs, M_I and M_V are the mobility of single interstitials and single vacancies characterized by the migration activation energy $E_m^{I,V}$ as $\nu\exp(-E_m^{I,V}/kT)$, and Z_S are the site numbers of the spontaneous reactions of each process. C_V is the vacancy concentration, C_L is the concentration of interstitial-type dislocation loops, C_{LI} is the concentration of interstitials already absorbed on the loops having a concentration of C_L, C_{void} is the concentration of voids, C_{VoidV} is the concentration of vacancies already absorbed on the voids having a concentration of C_{Void}, C_{CuV} is the concentration of copper-vacancy complexes, $C_{C\mathrm{CuV}}$ is the concentration of Cu cluster-vacancies complexes, and C_S is the concentration of permanent sinks, such as dislocations and grain boundaries. The second term on the right-hand side shows the mutual annihilation of single interstitials and vacancies. The third term is the formation of di-interstitials which are the nuclei of interstitial-type dislocation loops.[18] The fourth and fifth terms are interstitials annihilated with interstitial-type dislocation loops and voids, respectively. The sixth and seventh terms represent the annihilation of single interstitials at copper-vacancy complexes, Cu cluster-vacancies complexes, and permanent sinks, respectively.

C_V is expressed as:

$$dC_V/dt = P - Z_{IV}C_IC_V(M_I + M_V) - 2Z_{VV}M_VC_V^2 - Z_{LV}M_VC_V(C_{LI}C_L)^{1/2} - Z_{\mathrm{Void}V}M_VC_V(C_{\mathrm{Void}V}C_V)^{1/3} - Z_{V\mathrm{Cu}}M_VC_V(C_{\mathrm{Cu}} + C_{C\mathrm{Cu}} + C_{C\mathrm{CuV}}) - Z_{SV}M_VC_VC_S + \mathrm{EMIT}_{\mathrm{CuV}}C_{\mathrm{CuV}}. \quad (4)$$

As in Eq. (3), C_{Cu} is the concentration of Cu in the matrix, and $C_{C\mathrm{Cu}}$ the concentration of Cu clusters. The third term pertains to the formation of divacancies, which are the nuclei of vacancy clusters. The fourth and fifth terms are vacancies annihilated with interstitial-type dislocation loops and voids, respectively. The sixth and seventh terms correspond to the interactions between vacancies and copper atoms, Cu clusters, Cu cluster-vacancies complexes, and permanent sinks. The eighth term represents vacancies produced by the dissociation of copper-vacancy complexes. The probability of dissociation $\mathrm{EMIT}_{\mathrm{CuV}}$ varies with E_{emit} as $\nu\exp(-E_{\mathrm{emit}}/kT)$. Here, $E_{\mathrm{emit}}=E_m^V+E^b$. E^b is the binding energy between a Cu atom and a vacancy. On the basis of a molecular dynamics simulation, Ackland[19] calculated the binding energy of a single vacancy and Cu atom to be 0.087 eV when the Cu atom was at the nearest-neighbor site.

TABLE I. Parameters used in calculations.

P	1.2×10^{-8} dpa/s
E_m^I	0.3 eV
E_m^V	0.7 eV
T	573 K
E_{emit}	0.787 eV
C_S	10^{-10}
Z	1
ν	10^{13}
C_{Cu}	0.006

The concentration of Cu in the matrix of an Fe-Cu alloy, C_{Cu}, is expressed as:

$$dC_{Cu}/dt = Z_{I\mathrm{Cu}V}M_IC_IC_{\mathrm{CuV}} + \mathrm{EMIT}_{\mathrm{CuV}}C_{\mathrm{CuV}} - Z_{V\mathrm{Cu}}M_VC_V(C_{\mathrm{Cu}} + 2C_{\mathrm{Cu}}C_{\mathrm{Cu}} + C_{\mathrm{Cu}}C_{C\mathrm{CuV}}). \quad (5)$$

The first and second terms represent, respectively, the Cu produced by the recombination of interstitials and Cu-vacancy complexes and the dissociation of Cu-vacancy complexes. The third term pertains to the interactions of vacancies and copper atoms, the nuclei of Cu clusters, and Cu cluster-vacancies complexes. The parameters used in the present simulations are listed in Table I. The defect production rate, irradiation temperature, and Cu content in Fe were 1.2×10^{-8} dpa/s, 573 K, and 0.6 wt %, respectively, which were the same as in the irradiation experiments. In order to avoid the effect of site number Z on simulation results, site numbers for all reactions are set to be 1.

Figure 5 shows the concentration variation in Cu atoms,

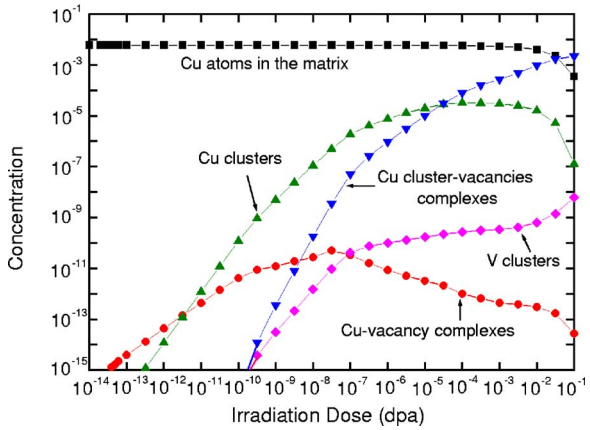

FIG. 5. (Color online) The concentration variation of Cu atoms in the matrix, Cu-vacancy complexes, Cu clusters, Cu cluster-vacancy complexes, and vacancy clusters during irradiation.

TABLE II. Influence of aggregation of Cu at microvoids on the positron-valence-electron (λ_v) and positron-core-electron (λ_c) annihilation rates. Relative weights of λ_c and λ_v in the total annihilation rate ($\lambda_c+\lambda_v$) are listed in parentheses. Schematic representation of Cu (dark spheres) and vacancy (white sphere) configurations is also in the list.

		λ_c (ns^{-1})	λ_v (ns^{-1})
Bcc Fe		1.17 (12.8%)	7.92 (81.2%)
Fe-1Cu-1V	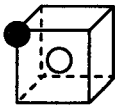	0.38 (6.7%)	5.29 (93.3%)
Fe-4Cu-1V	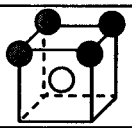	0.41 (7.1%)	5.32 (92.9%)
Fe-8Cu-1V	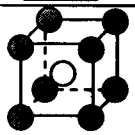	0.44 (7.5%)	5.41 (92.5%)

Cu-vacancy complexes, Cu clusters, Cu cluster-vacancies complexes, and vacancy clusters in the matrix during irradiation. The calculation indicates that vacancies produced by irradiation were trapped by Cu atoms to form Cu-vacancy complexes during the initial irradiation. Then, Cu clusters formed. The concentration of Cu clusters initially increased with the irradiation dose, and then decreased after irradiation to 5×10^{-3} dpa as the concentration of Cu atoms in the matrix decreased. The decrease in Cu cluster concentration was caused by the decrease in the formation of Cu clusters and increase in the formation of Cu cluster-vacancies complexes. As the concentration of Cu clusters, which were also trapping sites for vacancies, increased, Cu cluster-vacancies complexes formed. The concentration of Cu cluster-vacancies complexes increased with the irradiation dose. Finally, the vacancy clusters formed.

The concentration of vacancy clusters (vacancy clusters isolated from Cu precipitates in the matrix) was only 10^{-8} at 0.1 dpa, which means that vacancy clusters were not observed in the present experiments. Microvoids observed in the experiments were concluded to be vacancy clusters in Cu cluster-vacancies complexes. The formation of microvoids at Cu precipitates does not contradict the results of lifetime and CDB measurements. The shrinkage of microvoids observed at higher irradiation doses in the experiment, corresponding to a decrease in Cu cluster-vacancies complexes, was not simulated in the present calculation because the interaction potential between Fe and Cu was not considered.

IV. DISCUSSION

Our results clearly show that with increasing irradiation dose, Cu precipitated first, followed by the growth of microvoids near these precipitates, and then the evolution of precipitates and the shrinkage of microvoids started at the same time. The size of microvoids in metals and alloys seldom decreases during irradiation. For example, in the CDB results for pure Fe shown in Fig. 3, S increased with increasing irradiation dose as in many other metals and alloys, which corresponded to the growth of microvoids. Figure 4 shows that positrons trapped at microvoids were annihilated with core electrons in Cu. Moreover, the surface energy of Cu is lower than that of Fe.[20] These results lead us to conclude that Cu atoms are located on the microvoid surfaces when microvoids grow near Cu precipitates. This agrees with the conclusion by Nagai *et al.*[6] that Cu atoms aggregate on microvoid surfaces during annealing of Fe-Cu alloys irradiated with neutrons at 373 K. Although they also claimed that Cu precipitates were formed at the microvoid surfaces even during the irradiation, they did not provide supporting evidence.

S was different at points 3 and 3′ as shown in Fig. 3, while the lifetime of microvoids was the same (about 400 ps). There are two possible explanations for this contradiction. One is that a lifetime of 400 ps is almost the saturation value for microvoids.[21] Even if the microvoid size of Fe-0.6Cu is larger than that of Fe-0.3Cu, it is not detected by lifetime measurements. The other explanation is that according to the discussion above, Cu atoms aggregated prominently on the microvoid surfaces during irradiation from 3×10^{-3} dpa (3′) in Fe-0.6Cu, whereas aggregation of Cu atoms was significant during irradiation from 1.2×10^{-3} dpa (2) in Fe-0.3Cu. Thus, the microvoid environment was different at points 3 and 3′, namely, the aggregation of Cu atoms at the microvoid surfaces was more prominent at 3 than at 3′. The effects of the aggregation of Cu atoms at microvoids on the positron-valence-electron (λ_v) and positron-core-electron (λ_c) annihilation rates were investigated using the superposition method developed by Puska

and Nieminen.[14,22] The calculation results of bulk bcc Fe and single vacancy neighboring one Cu atom, four Cu atoms, and eight Cu atoms are shown in Table II. Here, the $3d4s$ electrons of Cu and Fe atoms were treated as the valence electrons. With an increasing number of Cu atoms around vacancies, the relative weight of λ_c increased, while that of λ_v decreased. This means that aggregation of Cu atoms at vacancies decreases S. Although our calculation is only for single vacancies, the same trend is expected in the case of microvoids, i.e., even if the size of microvoids is the same, S of microvoids surrounded by Cu atoms will be smaller than that surrounded by Fe.

V. CONCLUSION

Two Fe-Cu alloys—Fe-0.3Cu and Fe-0.6Cu—were irradiated with fission neutrons at doses from 4×10^{-4} to 6×10^{-3} dpa at 573 K to investigate Cu precipitation and microvoid evolution. The results of positron annihilation and simulation based on the rate theory indicate that there are three stages in the formation of Cu precipitates under the present irradiation conditions. First, the precipitates nucleate by vacancy migration. Second, microvoids form and grow at these precipitate sites. Third, the aggregation of Cu atoms is promoted at these microvoids. At the present irradiation doses, no void formation occurs in pure Fe.

An understanding of defect structure evolution is essential in designing alloys for nuclear applications. In the present Fe-Cu system, in which irradiation-induced precipitation occurs, it was found that the motion of point defects is affected by the alloying elements and precipitates, and consequently, the defect structure evolution varies greatly. The present study examined only the initial stage of irradiation. A future study will focus on the effect of the alloying elements at higher irradiation doses with an eye toward the development of nuclear materials to be used under high irradiation dose.

ACKNOWLEDGMENTS

We would like to express our thanks to E. Kuramoto and F. Hori for providing their software for calculation of positron and electron annihilation rates, and D. J. Bacon for his careful reading of the manuscript. This work was partly supported by a Grant-in-Aid for Scientific Research of the Ministry of Education, Science and Culture, under Contract No. 15560725.

[1] J. T. Buswell, C. A. English, M. G. Hetherington, W. J. Phythian, G. D. W. Smith, and G. M. Worrall, in *14th International Symposium, ASTM STP*, edited by N. H. Packan, R. E. Stoller, and A. S. Kumar (American Society for Testing and Materials, Philadelphia, 1990), Vol. II, p. 127.
[2] P. J. Othen, M. L. Jenkins, G. D. W. Smith, and W. J. Phythian, Philos. Mag. Lett. **64**, 383 (1991).
[3] W. J. Phythian and C. A. English, J. Nucl. Mater. **205**, 162 (1993).
[4] W. J. Phythian, A. J. E. Foreman, C. A. English, J. T. Buswell, M. Hetherington, K. Roberts, and S. Pizzini, ASTM Spec. Tech. Publ., **1125**, 131 (1992).
[5] R. Monzen, M. L. Jenkins, and A. P. Sutton, Philos. Mag. A **80**, 711 (2000).
[6] Y. Nagai, Z. Tang, M. Hassegawa, T. Kanai, and M. Saneyasu, Phys. Rev. B **63**, 134110 (2001).
[7] G. R. Odette, Scr. Metall. **17**, 1183 (1983).
[8] S. Yanagita, Ph. D. dissertation, Kyoto University, Japan, 2000.
[9] C. Zhang, M. Enomoto, T. Yamashita, and N. Sano, Metall. Mater. Trans. A **35**, 1263 (2004).
[10] A. Dupasquier and A. P. Mills, Jr., *Positron Spectroscopy of Solids* (IOS Press, Amsterdam, 1995).
[11] P. Asoka-Kumar, M. Alatalo, V. J. Ghosh, A. C. Kruseman, B. Nielsen, and K. G. Lynn, Phys. Rev. Lett. **77**, 2097 (1996).
[12] T. Yoshiie, Y. Hayashi, S. Yanagita, Q. Xu, Y. Satoh, H. Tsujimoto, T. Kozuka, K. Kamae, K. Mishima, S. Shiroya, K. Kobayashi, M. Utsuro, and Y. Fujita, Nucl. Instrum. Methods Phys. Res. A, **498**, 522 (2003).
[13] P. Kirkegaard, M. Eldrup, O. E. Morgensen, and N. J. Pedersen, Comput. Phys. Commun. **23**, 307 (1981).
[14] M. J. Puska and R. M. Nieminen, J. Phys. F: Met. Phys. **13**, 333 (1983).
[15] Q. Xu, H. Watanabe, and N. Yoshida, J. Nucl. Mater. **233**, 1057 (1996).
[16] N. Yoshida, Q. Xu, H. Watanabe, Y. Miyamoto, and T. Muroga, J. Nucl. Mater. **212**, 471 (1994).
[17] Z. Tang, M. Hasegawa, Y. Nagai, and M. Saito, Phys. Rev. B **65**, 195108 (2002).
[18] N. Yoshida, M. Kiritani, and F. E. Fujita, J. Phys. Soc. Jpn. **39**, 170 (1975).
[19] G. J. Ackland, D. J. Bacon, A. F. Calder, and T. Harry, Philos. Mag. A **75**, 713 (1997).
[20] L. Vitos, A. V. Ruban, H. L. Skriver, and J. Kollar, Surf. Sci. **411**, 186 (1998).
[21] A. Hempel, M. Saneyasu, Z. Tang, M. Hasegawa, G. Brauer, F. Plazaola, S. Yamaguchi, F. Kano, and A. Kawai, ASTM Spec. Tech. Publ. **1366**, 560 (2000).
[22] Y. Kamimura, T. Tsutsumi, and E. Kuramoto, Phys. Rev. B **52**, 879 (1995).